# A switching strategy for improving the performance of the frequency-domain block LMS algorithms for active noise control

Jun Wang, Jinpei Xue, and Jing Lu[a)]

*Key Laboratory of Modern Acoustics and Institute of Acoustics, Nanjing University, Nanjing 210093, China*

Xiaojun Qiu

*Centre for Audio, Acoustics and Vibration, Faculty of Engineering and Information Technology, University of Technology Sydney, NSW 2007, Australia*

[a)] Electronic mail: lujing@nju.edu.cn

Running title: Improved adaptive algorithm

**Abstract:** The bin-normalized frequency domain block LMS (NFBLMS) algorithm demonstrates high convergence speed in active noise control (ANC) applications; however, it suffers from a biased steady-state solution when the adaptive filter length is not sufficient. A modified FBLMS (MFBLMS) algorithm has been proposed recently to solve the problem with guaranteed optimal steady-state performance, but its convergence speed is lower than that of the NFBLMS algorithm. In this paper, an improved algorithm is proposed by combining the NFBLMS and MFBLMS algorithms. Based on the analysis of the initial convergence trajectory of the NFBLMS algorithm, an effective switching strategy is designed, which enables the MFBLMS algorithm after the NFBLMS algorithm approaches its steady state and switches back to the NFBLMS algorithm when an environmental change is detected. The simulation results using the measured acoustic transfer functions are presented to demonstrate that the proposed algorithm gains both high convergence speed and optimal steady-state performance from the NFBLMS and MFBLMS algorithms.

**Keywords:** active noise control; frequency domain adaptive algorithm; insufficient filter length.

## I. INTRODUCTION

Active noise control (ANC) has wide applications in sound barriers, cars and headphones[0-4] due to its benefits of attenuating low-frequency noise without bulky passive structures. For the common feedforward control system, the filtered-x LMS (FXLMS) algorithm is widely utilized because of its simplicity and stability.[5-10] However, as noted by many researchers, the time domain FXLMS algorithm suffers from low convergence speed.[11] Many effective alternatives, such as the frequency domain block least mean square (FBLMS) algorithm, [12-15] subband algorithm,[16,17] and variable step size (VSS) algorithm,[18] have been proposed.

The normalized FBLMS (NFBLMS) algorithm, obtained by normalizing the stepsize of the FBLMS algorithm according to the reference signal power in each frequency bin, theoretically has a uniform convergence mode in each frequency bin.[19,20] Although the NFBLMS algorithm has high convergence speed for colored noise, its mean squared error (MSE) is large with insufficient adaptive filter length, which is a common scenario in ANC system due to the existence of the secondary path between the control source and the error sensor. [21,22,23] A modified FBLMS (MFBLMS) algorithm has been proposed, which can guarantee the optimal steady-state behavior at cost of some computational complexcities.[24] Unfortunately, the convergence speed of the MFBLMS algorithm has been found to be generally lower than that of the NFBLMS algorithm.[25]

In this paper, a quantitative analysis of the initial convergence behavior of the NFBLMS algorithm is presented first, and then a switching mechanism between the NFBLMS and the MFBLMS algorithms is designed based on this. The benefits of both the NFBLMS and the MFBLMS algorithms are combined in the proposed algorithm, ensuring both the high convergence speed and the optimal steady-state behavior. Simulations with the measured ANC transfer functions are carried out to validate the efficacy of the proposed algorithm.

Throughout this paper, lowercase letters are used for scalar quantities, bold lowercase for vectors and bold uppercase for matrices. Subscript f denotes a frequency domain representation of each signal and $k$ is reserved for the block index.

## II. THE FREQUENCY DOMAIN ALGORITHM

A block diagram of a common feedforward ANC system is shown in Figure 1, where $H_r(z)$ is the transfer function from the noise source to the reference sensor, $H_p(z)$ and $H_s(z)$ are the transfer functions of the primary and the secondary paths, $\hat{H}_s(z)$ is the modeled secondary path transfer function, and $W(z)$ is the control filter.

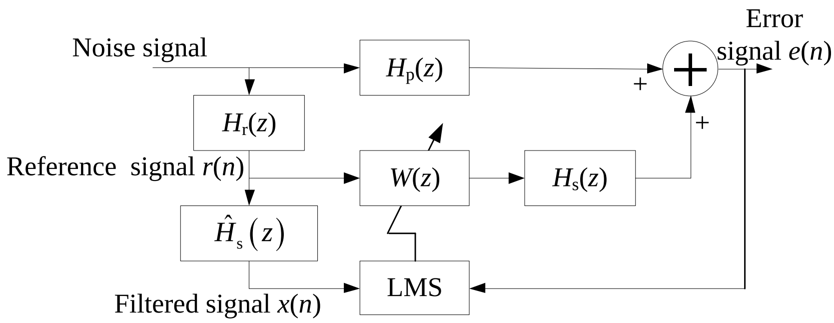


Figure 1. Block diagram of the FxLMS algorithm

To reduce the computational complexity and increase the convergence speed, the NFBLMS[15] and MFBLMS[24] algorithms can be applied in the ANC system. If the secondary path is perfectly modeled, i.e., $\hat{H}_s(z) = H_s(z)$, the frequency domain algorithm for ANC can be simplified as the adaptive system identification algorithm,[21] as shown in Figure 2, where $\mathbf{x}(k)$ and $\mathbf{e}(k)$ denote the filtered signal vector and the error signal vector in the time domain respectively, $\mathbf{x}_f(k)$ and $\mathbf{e}_f(k)$ denote the filtered signal vector and the error signal vector in the frequency domain respectively, $\mathbf{w}_f(k)$ is the control filter in the frequency domain, and $\boldsymbol{\xi}$ is the vector containing the normalizing factors for each frequency bin. The length of the control filter is $N$, and the block length of the algorithm is usually also set as $N$, so the length of the DFT operation is $2N$. The red line and the blue line indicate the signal flow of the NFBLMS and MFBLMS algorithms, respectively. The black line indicates the signal flow of both algorithms.

The commonly used update equation of the constrained NFBLMS algorithm is [24]

$$\mathbf{w}_{\mathrm{f}}\left(k+1\right)=\mathbf{w}_{\mathrm{f}}\left(k\right)+2\mu\mathbf{Q}_{N,0}\mathbf{M}_{\mathrm{f}}\mathbf{X}_{\mathrm{f}}^{\mathrm{H}}\left(k\right)\mathbf{e}_{\mathrm{f}}\left(k\right), \tag{1}$$

where the superscript H represents the conjugate transpose operation, $\mu$ is step size normalized by $\boldsymbol{\xi}$, $\mathbf{X}_{\mathrm{f}}(k) = \mathrm{diag}[\mathbf{x}_{\mathrm{f}}(k)]$, $\mathbf{M}_{\mathrm{f}} = \mathrm{diag}[\boldsymbol{\xi}]$, and $\boldsymbol{\xi}$ is usually set as the reciprocal of the reference signal power, so that

$$\mathbf{M}_{\mathrm{f}}=\left\{E\left[\mathbf{X}_{\mathrm{f}}^{\mathrm{H}}\left(k\right)\mathbf{X}_{\mathrm{f}}\left(k\right)\right]\right\}^{-1}. \tag{2}$$

$\mathbf{Q}_{N,0} = \mathbf{F}\mathbf{G}_{N,0}\mathbf{F}^{-1}$, $\mathbf{Q}_{0,N} = \mathbf{F}\mathbf{G}_{0,N}\mathbf{F}^{-1}$, $\mathbf{F}$ represents a $2N\times 2N$ discrete Fourier transform (DFT) matrix, and

$$\mathbf{G}_{N,0}=\begin{bmatrix}\mathbf{I}_{N\times N} & \mathbf{0}_{N\times N}\\ \mathbf{0}_{N\times N} & \mathbf{0}_{N\times N}\end{bmatrix},\mathbf{G}_{0,N}=\begin{bmatrix}\mathbf{0}_{N\times N} & \mathbf{0}_{N\times N}\\ \mathbf{0}_{N\times N} & \mathbf{I}_{N\times N}\end{bmatrix}. \tag{3}$$

The filter update equation of the MFBLMS algorithm is given by[24]

$$\mathbf{w}_{\mathrm{f}}\left(k+1\right)=\mathbf{w}_{\mathrm{f}}\left(k\right)+2\mu\mathbf{Q}_{N,0}\mathbf{M}_{\mathrm{f}}\mathbf{Q}_{N,0}\mathbf{X}_{\mathrm{f}}^{\mathrm{H}}\left(k\right)\mathbf{e}_{\mathrm{f}}\left(k\right). \tag{4}$$

The difference between Eqs. (1) and (4) is that there is one more $\mathbf{Q}_{N,0}$ in Eq. (4).

When the adaptive filter is of insufficient length, the steady-state solution of the NFBLMS algorithm deviates from the optimal Wiener solution while the MFBLMS algorithm remains converging to the Wiener solution.[26] However, the convergence speed of the MFBLMS algorithm has been found to be slower than that of the NFBLMS algorithm due to …..[25] Therefore it is reasonable to combine the high convergence speed of the NFBLMS algorithm and the optimal steady-state behavior of the MFBLMS algorithm, and the key is to design an effective switching strategy.

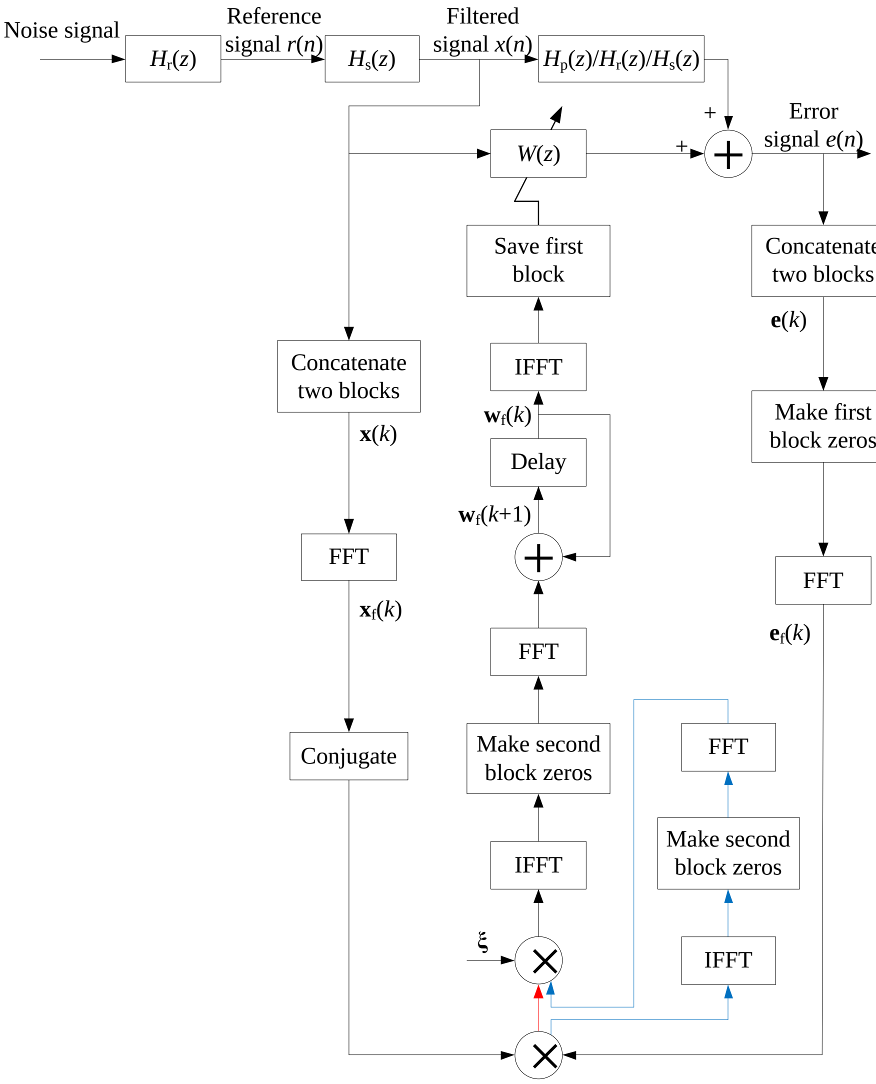


Figure 2. Block diagram of the NFBLMS (red) and MFBLMS (blue) algorithms

## III. THE PROPOSED ALGORITHM

In the NFBLMS algorithm, it has [26]

$$\begin{aligned}\mathbf{v}_f(k+1) = &\left[\mathbf{I} - 2\mu \mathbf{Q}_{N,0}\mathbf{M}_f\mathbf{X}_f^{H}(k)\mathbf{Q}_{0,N}\mathbf{X}_f(k)\right]\mathbf{v}_f(k)\\ &+2\mu \mathbf{Q}_{N,0}\mathbf{M}_f\mathbf{X}_f^{H}(k)\mathbf{Q}_{0,N}\mathbf{e}_{f,o}(k)\end{aligned}, \quad (5)$$

where $\mathbf{v}_f(k) = \mathbf{w}_f(k) - \mathbf{w}_{f,o}(k)$, $\mathbf{w}_{f,o}(k)$ is the steady-state adaptive filter in the frequency domain, and $\mathbf{e}_{f,o}(k)$ is the steady-state error in the frequency domain. It is usually assumed that the elements of the frequency bins of the filtered signal behave like independent complex Gaussian stationary random variables,[27] whose modulus square satisfies a chi-square distribution with 2 degrees of freedom.[28] $E[\mathbf{Q}_{N,0}\mathbf{M}_\mathrm{f}\mathbf{X}_\mathrm{f}^\mathrm{H}(k)\mathbf{Q}_{0,N}\mathbf{e}_\mathrm{f,o}(k)] = 0$, $\mathbf{Q}_{N,0} \approx \mathbf{I}/2$ and $\mathbf{Q}_{0,N} \approx \mathbf{I}/2$ for large enough $N$, $E[\mathbf{Q}_{N,0}\mathbf{M}_\mathrm{f}\mathbf{X}_\mathrm{f}^\mathrm{H}(k)\mathbf{Q}_{0,N}\mathbf{X}_\mathrm{f}(k)] \approx \mathbf{I}/4$, and $\mathbf{Q}_{N,0}\mathbf{M}_\mathrm{f}\mathbf{X}_\mathrm{f}^\mathrm{H}(k)\mathbf{Q}_{0,N}\mathbf{X}_\mathrm{f}(k)$ is approximated as a diagonal matrix.[19]

To confirm the analysis results, Figure 3 shows the value distribution $\mathbf{Q}_{0,N}$ and $\mathbf{Q}_{N,0}\mathbf{M}_\mathrm{f}\mathbf{X}_\mathrm{f}^\mathrm{H}(k)\mathbf{Q}_{0,N}\mathbf{X}_\mathrm{f}(k)$ when $N = 2048$, with noise signal generated by passing the Gaussian white noise through the transfer function $H(z) = (1-0.5z^{-1})^{10}/(1-0.6z^{-1})^{10}$. It is clear that both matrices are close to an ideal diagonal matrix, and the diagonal element of $\mathbf{Q}_{0,N}$ is around 0.5 while the diagonal element of $\mathbf{Q}_{N,0}\mathbf{M}_\mathrm{f}\mathbf{X}_\mathrm{f}^\mathrm{H}(k)\mathbf{Q}_{0,N}\mathbf{X}_\mathrm{f}(k)$ is around 0.25, as anticipated from the analysis.

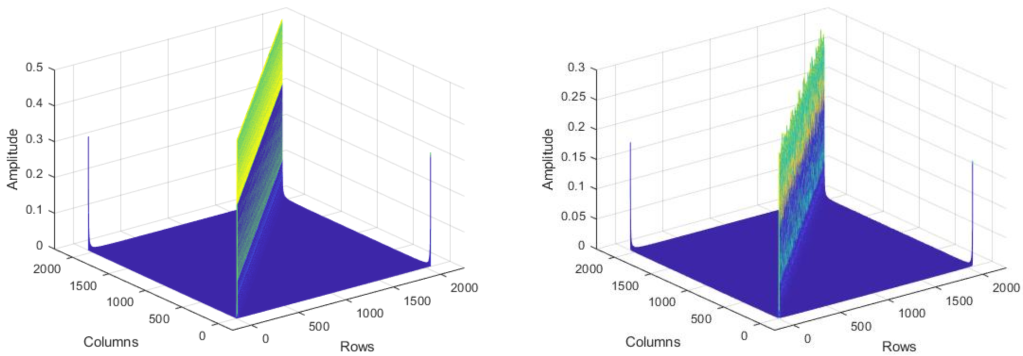


(a) (b)

Figure 3. Distribution of matrix coefficients with (a) $\mathbf{Q}_{0,N}$; (b) $\mathbf{Q}_{N,0}\mathbf{M}_\mathrm{f}\mathbf{X}_\mathrm{f}^\mathrm{H}(k)\mathbf{Q}_{0,N}\mathbf{X}_\mathrm{f}(k)$.

Let

$$\mathbf{\Phi}(k) = 2\mathbf{Q}_{N,0}\mathbf{M}_\mathrm{f}\mathbf{X}_\mathrm{f}^\mathrm{H}(k)\mathbf{Q}_{0,N}\mathbf{X}_\mathrm{f}(k). \tag{6}$$

When the initial value of the adaptive filter is far enough away from the steady-state solution, $\mu\mathbf{Q}_{N,0}\mathbf{M}_\mathrm{f}\mathbf{X}_\mathrm{f}^\mathrm{H}(k)\mathbf{Q}_{0,N}\mathbf{e}_\mathrm{f,o}(k)$ is considerably smaller than $\mathbf{v}_\mathrm{f}(k)$ at the initial stage of the filter updating process and is negligible. Substituting Eq. (6) in Eq. (5) yields

$$\mathbf{v}_\mathrm{f}(k+1) = \left[\mathbf{I} - \mu\mathbf{\Phi}(k)\right]\mathbf{v}_\mathrm{f}(k). \tag{7}$$

The error of the NFBLMS and MFBLMS algorithms can both be described as[24]

$$\mathbf{e}_\mathrm{f}(k) = \mathbf{Q}_{0,N}\left[\mathbf{d}_\mathrm{f}(k) - \mathbf{X}_\mathrm{f}(k)\mathbf{w}_\mathrm{f}(k)\right], \tag{8}$$

where $\mathbf{d}_\mathrm{f}(k)$ is the desired signal in the frequency domain. It can be seen from Eq. (8) that

$$\begin{aligned}\mathbf{e}_\mathrm{f}(k) &= \mathbf{Q}_{0,N}\left[\mathbf{X}_\mathrm{f}(k)\mathbf{w}_\mathrm{f,o}(k) + \mathbf{e}_\mathrm{f,o}(k) - \mathbf{X}_\mathrm{f}(k)\mathbf{w}_\mathrm{f}(k)\right] \\ &= -\mathbf{Q}_{0,N}\mathbf{X}_\mathrm{f}(k)\mathbf{v}_\mathrm{f}(k) + \mathbf{Q}_{0,N}\mathbf{e}_\mathrm{f,o}(k)\end{aligned}. \tag{9}$$

When the initial value of the adaptive filter is far away from the steady-state solution, $\mathbf{e}_\mathrm{f}(k) - \mathbf{Q}_{0,N}\mathbf{e}_\mathrm{f,o}(k) \approx \mathbf{e}_\mathrm{f}(k)$ at the initial stage. Eq. (9) can be simplified as

$$\mathbf{e}_\mathrm{f}(k) = -\mathbf{Q}_{0,N}\mathbf{X}_\mathrm{f}(k)\mathbf{v}_\mathrm{f}(k). \tag{10}$$

According to the independence assumption,[20] $\mathbf{v}_\mathrm{f}(k)$ is only related to the past observations and is independent of the information of the current block. Multiplying both sides of Eq. (10) with their respective conjugate transpositions and then taking expectation leads to

$$\begin{aligned}E\left[\mathbf{e}_\mathrm{f}^\mathrm{H}(k)\mathbf{e}_\mathrm{f}(k)\right] &= E\left[\mathbf{v}_\mathrm{f}^\mathrm{H}(k)\mathbf{X}_\mathrm{f}^\mathrm{H}(k)\mathbf{Q}_{0,N}^\mathrm{H}\mathbf{Q}_{0,N}\mathbf{X}_\mathrm{f}(k)\mathbf{v}_\mathrm{f}(k)\right] \\ &= E\left\{\mathbf{v}_\mathrm{f}^\mathrm{H}(k)E\left[\mathbf{X}_\mathrm{f}^\mathrm{H}(k)\mathbf{Q}_{0,N}^\mathrm{H}\mathbf{Q}_{0,N}\mathbf{X}_\mathrm{f}(k)\right]\mathbf{v}_\mathrm{f}(k)\right\}\end{aligned}. \tag{11}$$

Let $J_\mathrm{m}(k) = E[\mathbf{e}_\mathrm{f}^\mathrm{H}(k)\mathbf{e}_\mathrm{f}(k)]$, substituting Eq. (7) in Eq. (11) yields

$$\begin{aligned}&J_\mathrm{m}(k+1) \\ &= E\left[\mathbf{e}_\mathrm{f}^\mathrm{H}(k+1)\mathbf{e}_\mathrm{f}(k+1)\right] \\ &= E\left\{\mathbf{v}_\mathrm{f}^\mathrm{H}(k)\left[\mathbf{I} - \mu\mathbf{\Phi}^\mathrm{H}(k)\right]E\left[\mathbf{X}_\mathrm{f}^\mathrm{H}(k+1)\mathbf{Q}_{0,N}^\mathrm{H}\mathbf{Q}_{0,N}\mathbf{X}_\mathrm{f}(k+1)\right]\left[\mathbf{I} - \mu\mathbf{\Phi}(k)\right]\mathbf{v}_\mathrm{f}(k)\right\}\end{aligned}. \tag{12}$$

Since $\mathbf{\Phi}(k)$ is only related to $\mathbf{X}_\mathrm{f}(k)$, $\mathbf{\Phi}(k)$ is independent of $\mathbf{X}_\mathrm{f}(k+1)$ due to the independence assumption. Note the matrices in Eq. (12) are all approximated as diagonal matrices, so Eq. (12) can be expressed as

$$\begin{aligned}&J_\mathrm{m}(k+1) \\ &= E\left\langle\mathbf{v}_\mathrm{f}^\mathrm{H}(k)E\left\{\left[\mathbf{I} - \mu\mathbf{\Phi}^\mathrm{H}(k)\right]E\left[\mathbf{X}_\mathrm{f}^\mathrm{H}(k+1)\mathbf{Q}_{0,N}^\mathrm{H}\mathbf{Q}_{0,N}\mathbf{X}_\mathrm{f}(k+1)\right]\left[\mathbf{I} - \mu\mathbf{\Phi}(k)\right]\right\}\mathbf{v}_\mathrm{f}(k)\right\rangle \\ &= E\left\{\mathbf{v}_\mathrm{f}^\mathrm{H}(k)E\left[\mathbf{I} - \mu\mathbf{\Phi}^\mathrm{H}(k)\right]\left[\mathbf{I} - \mu\mathbf{\Phi}(k)\right]E\left[\mathbf{X}_\mathrm{f}^\mathrm{H}(k+1)\mathbf{Q}_{0,N}^\mathrm{H}\mathbf{Q}_{0,N}\mathbf{X}_\mathrm{f}(k+1)\right]\mathbf{v}_\mathrm{f}(k)\right\}\end{aligned}.$$

(13)

Known by the characteristics of the chi-square distribution,[29] $E[\mathbf{\Phi}(k)] = 0.5\mathbf{I}$ and $E\{[\mathbf{\Phi}^{\mathrm{H}}(k) - 0.5\mathbf{I}][\mathbf{\Phi}(k) - 0.5\mathbf{I}]\} \approx 0.25\mathbf{I}$, then

$$\begin{aligned}
&E\left\{\left[\mathbf{I}-\mu\mathbf{\Phi}^{\mathrm{H}}(k)\right]\left[\mathbf{I}-\mu\mathbf{\Phi}(k)\right]\right\} \\
&=E\left\langle\left\{\left(1-\frac{\mu}{2}\right)\mathbf{I}-\mu\left[\mathbf{\Phi}^{\mathrm{H}}(k)-\frac{1}{2}\mathbf{I}\right]\right\}\left\{\left(1-\frac{\mu}{2}\right)\mathbf{I}-\mu\left[\mathbf{\Phi}(k)-\frac{1}{2}\mathbf{I}\right]\right\}\right\rangle \\
&=\left(1-\frac{\mu}{2}\right)^2\mathbf{I}+\mu^2E\left\{\left[\mathbf{\Phi}^{\mathrm{H}}(k)-\frac{1}{2}\mathbf{I}\right]\left[\mathbf{\Phi}(k)-\frac{1}{2}\mathbf{I}\right]\right\} \\
&=\left[\left(1-\frac{\mu}{2}\right)^2+\frac{\mu^2}{4}\right]\mathbf{I}=b\mathbf{I}
\end{aligned}, \tag{14}$$

where $b = (1 - \mu / 2)^2 + \mu^2 / 4$.

According to the independence assumption, $\mathbf{v}_{\mathrm{f}}(k)$ is independent of $\mathbf{\Phi}(k)$. Assume that the noise is stationary, then substituting Eq. (14) in Eq. (13) leads to

$$\begin{aligned}
&J_{\mathrm{m}}(k+1) \\
&=bE\left\{\mathbf{v}_{\mathrm{f}}^{\mathrm{H}}(k)E\left[\mathbf{X}_{\mathrm{f}}^{\mathrm{H}}(k+1)\mathbf{Q}_{0,N}^{\mathrm{H}}\mathbf{Q}_{0,N}\mathbf{X}_{\mathrm{f}}(k+1)\right]\mathbf{v}_{\mathrm{f}}(k)\right\} \\
&=bE\left\{\mathbf{v}_{\mathrm{f}}^{\mathrm{H}}(k)E\left[\mathbf{X}_{\mathrm{f}}^{\mathrm{H}}(k)\mathbf{Q}_{0,N}^{\mathrm{H}}\mathbf{Q}_{0,N}\mathbf{X}_{\mathrm{f}}(k)\right]\mathbf{v}_{\mathrm{f}}(k)\right\} \\
&=bE\left[\mathbf{e}_{\mathrm{f}}^{\mathrm{H}}(k)\mathbf{e}_{\mathrm{f}}(k)\right] \\
&=bJ_{\mathrm{m}}(k)
\end{aligned}. \tag{15}$$

In practice, $J_{\mathrm{m}}(k)$ is initialized using the instantaneous squared error $J(k) = \mathbf{e}_{\mathrm{f}}^{\mathrm{H}}(k)\mathbf{e}_{\mathrm{f}}(k)$ and the update process is carried out as

$$J_{\mathrm{m}}(k)=bJ_{\mathrm{m}}(k-1)+\alpha\left[J(k)-bJ_{\mathrm{m}}(k-1)\right], \tag{16}$$

where $\alpha$ is a small regularization coefficient to mitigate the variation of the instantaneous estimate. It can be expected that $J_{\mathrm{m}}(k)$ decreases fast at the initial stage and remains comparatively stable when the filter approaches the steady-state. Therefore a reasonable criterion to determine the convergence state of the NFBLMS algorithm is to calculate the difference of $J_{\mathrm{m}}(k)$ as $\varDelta_{\mathrm{J}}(k) = J_{\mathrm{m}}(k-1) - J_{\mathrm{m}}(k)$. When $\varDelta_{\mathrm{J}}(k)$ is smaller than a preset threshold $\varDelta^{\mathrm{THR}}$, the NFBLMS algorithm reaches the steady-state and the proposed algorithm should switch to the MFBLMS algorithm.

When the secondary path is fixed but the position of the noise source or the reference sensor changes, the control process needs to switch back to the NFBLMS algorithm to guarantee a higher convergence speed. The steady-state tracking parameter is set as

$$\zeta\left(k\right)=\frac{E\left(\mathbf{e}_{\mathrm{f}}\left(k\right)^{\mathrm{T}}\mathbf{Q}_{0,N}\mathbf{e}_{\mathrm{f}}\left(k\right)\right)}{E\left(\mathbf{x}_{\mathrm{f}}\left(k\right)^{\mathrm{T}}\mathbf{Q}_{0,N}\mathbf{x}_{\mathrm{f}}\left(k\right)\right)}. \tag{17}$$

When $\zeta(k)$ suddenly increases above a threshold $\zeta^{\mathrm{THR}}$, the ANC system needs to be re-initialized to the NFBLMS algorithm.

The schematic diagram of the switching strategy is shown in Figure 4. To prevent frequent switching between the two algorithms, each algorithm needs to run continuously at least for $M$ blocks after a switch. The proposed algorithm is initialized with the NFBLMS algorithm. When $\Delta_{\mathrm{J}}(k) < \Delta^{\mathrm{THR}}$, the NFBLMS algorithm is assumed to reach steady-state, and the proposed algorithm is switched to the MFBLMS algorithm. When the MFBLMS algorithm converges close to the Wiener solution, $\zeta(k)$ fluctuates around the minimum value. In order to set a reasonable $\zeta^{\mathrm{THR}}$, the proposed algorithm switches to the NFBLMS algorithm for a short while and obtains a larger $\zeta(k)$ that can be set as $\zeta^{\mathrm{THR}}$. After that, the proposed algorithm switches back to the MFBLMS algorithm. When $\zeta(k) > \zeta^{\mathrm{THR}}$, a considerable change of the acoustic environment is detected and the proposed algorithm switches to the NFBLMS algorithm for a high convergence speed.

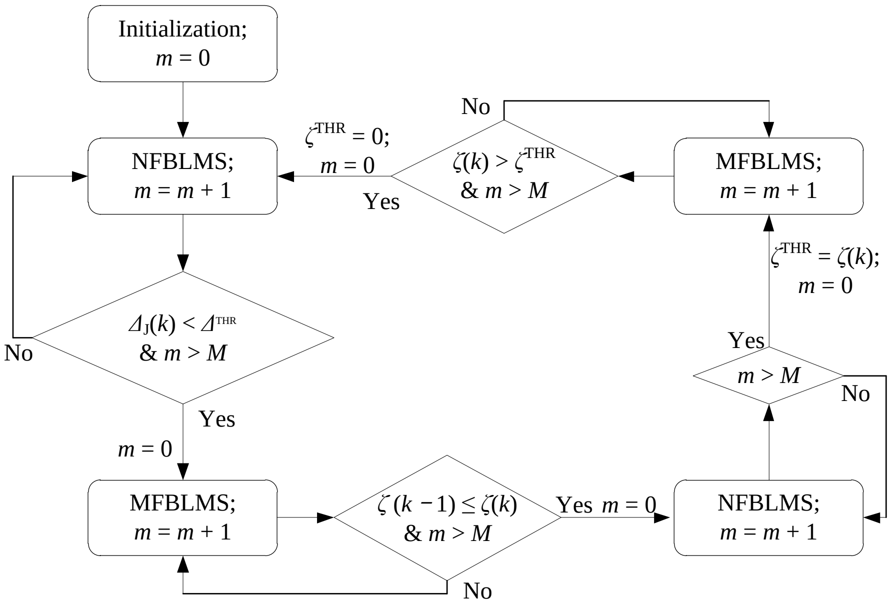


Figure 4. The switching strategy of the proposed algorithm.

In the proposed frequency-domain algorithm, the high convergence speed of the NFBLMS algorithm and the optimal steady-state behavior of the MFBLMS algorithm are combined efficiently with a limited increase of the computational burden. Furthermore, the proposed algorithm can also track the variation of the acoustic environment and re-converges efficiently when the position of the noise source or the reference sensor is changed.

## IV. SIMULATIONS

The performance of the proposed algorithm is demonstrated by comparing with the ANC systems based only on the NFBLMS or the MFBLMS algorithms with the measured data. The measurements were conducted in a normal room with a sampling rate of 16 kHz, where the noise signal is generated by passing the Gaussian white noise through a low-pass filter $H(z)$ with cut-off frequency of 6 kHz, as shown in Figure 5.

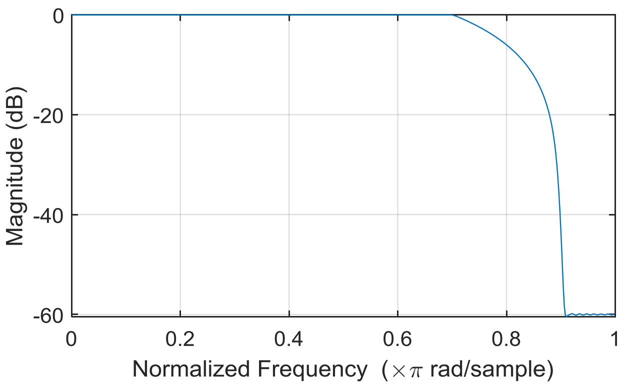


Figure 5 Frequency response of $H(z)$ used in the measurements.

The noise source was placed in two positions shown in Figure 6, resulting in different reference transfer functions, $H_{r1}(z)$ and $H_{r2}(z)$, and different primary transfer functions, $H_{p1}(z)$ and $H_{p2}(z)$. All the measured impulse responses, including $H_s(z)$, are shown in Figure 7. The acoustics feedback from the control source to the reference sensor is removed with feedback neutralization.[错误!未找到引用源。]

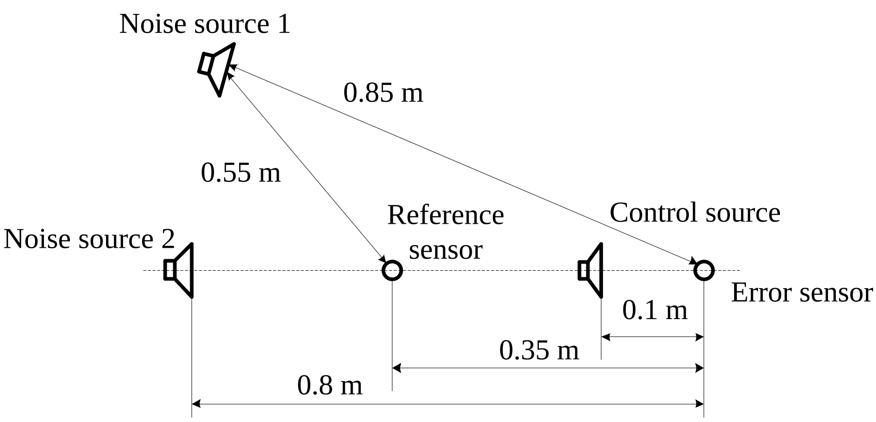


Figure 6. The positions of sources and sensors in the measurements.

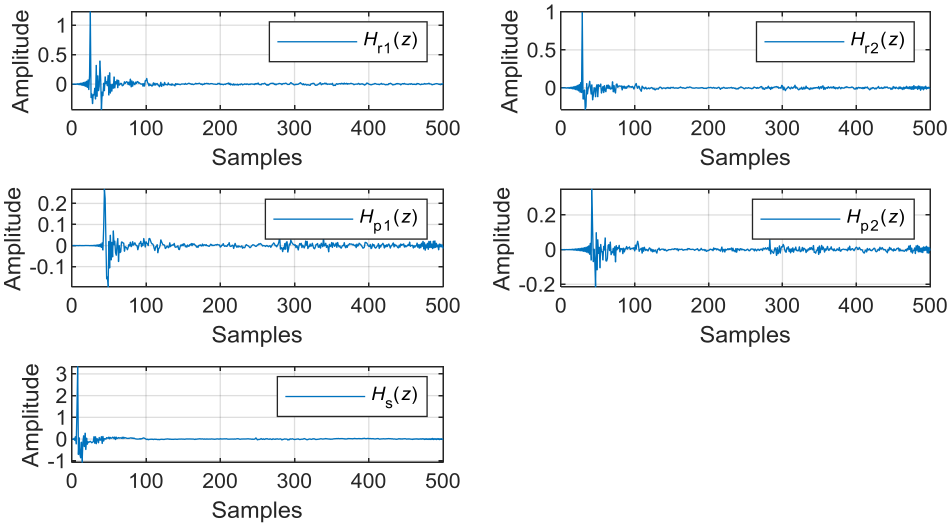


Figure 7. The impulse responses used in the measurements.

The measurement data is divided into two sections. The first section is obtained with the noise source 1, and the second section is obtained with the noise source 2. The control filter length is set as 1024, the signal block length is 1024 and the FFT of 2048 points is utilized in the proposed algorithm. The step sizes of all algorithms are set to guarantee both the high convergence speed and the stability of the system. The results are averaged over 10 independent trials. The comparison of the convergence of the three algorithms in the ANC system is shown in Figure 8.

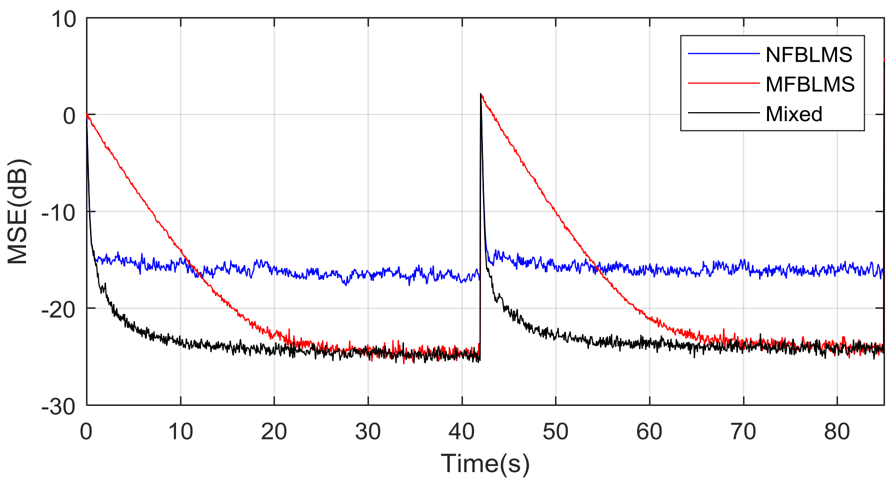

Figure 8. The convergence curves of the three algorithms

In Figure 8, the NFBLMS algorithm convergences faster to a biased steady-state within 0.7 s, while the MFBLMS algorithm suffers from significantly longer convergence time but with a much lower MSE. The proposed algorithm switches effectively to the MFBLMS algorithm at about 1.0 s and converges to the lower MSE. This demonstrates clearly the benefit of the combination of both the NFBLMS algorithm and the MFBLMS algorithm. When the position of the noise source is changed at 42 s, the noise control performance of all the three algorithms deteriorate quickly as expected. Then the proposed algorithm switched to the NFBLMS algorithm to have fast convergence speed. When the NFBLMS algorithm approaches the steady-state, the MFBLMS algorithm is again launched, resulting in a lower residual noise than that achieved by the NFBLMS algorithm.

## V. CONCLUSIONS

An improved active noise control algorithm combining the benefits of the NFBLMS and MFBLMS algorithms is proposed based on an effective switching strategy between these two algorithms. The proposed algorithm launches the NFBLMS algorithm initially and switches to the MFBLMS algorithm when the NFBLMS algorithm converges close to its steady state, resulting in both high convergence speed and optimal steady-state performance of the system. Simulations using real measured acoustic impulse responses validate the efficacy of the proposed algorithm in a feedforward active noise control system.

## ACKNOWLEDGEMENTS

This work was supported by the National Natural Science Foundation of China (Grant No.11874219).

## REFERENCES


1. C. Hansen, S. Snyder and X. Qiu, et al., "Active Control of Noise and Vibration, Second Edition," (Crc Press, London, 2012).
2. Y. Kajikawa, W. S. Gan and S. M. Kuo, "Recent advances on active noise control: open issues and innovative applications," APSIPA Trans. Signal Info. Process. **1**, 1-21 (2012).
3. S. Kuo, Y. R. Chen and C. Y. Chang, et al., "Development and Evaluation of Light-Weight Active Noise Cancellation Earphones," Appl. Sci. **8**(7), 1178 (2018).
4. S. K. Lee, S. Lee and J. Back, et al., "A New Method for Active Cancellation of Engine Order Noise in a Passenger Car," Appl. Sci. **8**(8), 1394 (2018).
5. M. R. Bai, Y. Lin and J. Lai, "Reduction of electronic delay in active noise control systems— A multirate signal processing approach," J. Acoust. Soc. Am. **111**(2), 916-924 (2002).
6. Cheer and Jordan, "Active control of scattered acoustic fields: Cancellation, reproduction and cloaking," J. Acoust. Soc. Am. **140**(3), 1502-1512 (2016).
7. J. Wang, J. Lu, and X. Qiu, "A compact active sound absorption system compensating near-field effect of the secondary source," Noise Control Eng. J. **65**(5), 482-487 (2017).
8. K. Iwai, S. Hase and Y. Kajikawa, "Multichannel Feedforward Active Noise Control System with Optimal Reference Microphone SelectorBased on Time Difference of Arrival," Appl. Sci. **8**(11), 2291 (2018).
9. M. R. Bai, W. Pan and H. Chen, "Active feedforward noise control and signal tracking of headsets: Electroacoustic analysis and system implementation," J. Acoust. Soc. Am. **143**(3), 1613-1622 (2018).
10. H. Wang, et al., "A multi-tone active noise control system with a simplified local on-line secondary-path modeling," J. Acoust. Soc. Am. **144**(6), EL515-521 (2018).

11. B. Widrow, J. M. Mccool and M. G. Larimore, et al., "Stationary and nonstationary learning characteristics of the LMS adaptive filter," Proc. IEEE. **64**(8), 1151-1162 (1976).

12. D. P. Das, G. Panda and S. M. Kuo, "New block filtered-X LMS algorithms for active noise control systems," IET Signal Process. **1**(2), 73-81 (2007).

13. X. Qiu and C. Hansen, "Multidelay adaptive filters for active noise control," In Proc. 14th Int. Congr. Sound Vibr. (ICSV), Cairns, Australia, 724-732 (2007).

14. J. Lorente, M. Ferrer and M. D. Diego, et al., "GPU Implementation of Multichannel Adaptive Algorithms for Local Active Noise Control," IEEE/ACM Trans. Audio Speech Lang. Process. **22**(11), 1624-1635 (2014).

15. F. Yang, Y. Cao and M. Wu, et al., "Frequency-Domain Filtered-x LMS Algorithms for Active Noise Control: A Review and New Insights," Appl. Sci. **8**(11), 2313 (2018).

16. K. A. Lee. W. S. Gan and S. M. Kuo, "Subband adaptive filtering: theory and implementation," (John Wiley & Sons, New York, 2009).

17. M. Gao, J. Lu and X. Qiu, "A simplified subband ANC algorithm without secondary path modeling," IEEE Trans. Speech Audio Process. **24**(7), 1164-1174 (2016).

18. Y. Sun, M. Wang and Y. Han, et al., "An improved VSS NLMS algorithm for active noise cancellation," AIP Conf. Proc. **1864**(1), 020158 (2016).

19. B. Farhang-Boroujeny and K. S. Chan, "Analysis of the frequency-domain block LMS algorithm," IEEE Trans. Signal Process. **48**(8), 2332-2342 (2000).

20. B. Farhang-Boroujeny, "Adaptive Filters: Theory and Applications 2nd Edition," (John Wiley & Sons, New York, 2013).

21. S. Elliott, "Signal Processing for Active Control," (Academic Press, London, 2000).

22. M. Wu, J. Yang, Y. Xu and X. Qiu, "Steady-state solution of the deficient length constrained FBLMS algorithm," IEEE Trans. Signal Process. **60**, 6681-6687 (2012).

23. L. Zhang and X. Qiu, "Causality study on a feedforward active noise control headset with different noise coming directions in free field," Appl. Acoust. **80**, 36-44 (2014).

24. J. Lu, X. Qiu and H. S. Zou, "A modified frequency-domain block LMS algorithm with guaranteed optimal steady-state performance," Signal Process. **104**, 27-32 (2014).

25. J. Lu, K. Chen, and X. Qiu, "Convergence analysis of the modified frequency-domain block LMS algorithm with guaranteed optimal steady state performance," Signal Process. **132**, 165-169 (2017).

26. M. Wu and J. Yang, "A step size control method for deficient length FBLMS algorithm," IEEE Signal Process. Let. **22**(9), 1448-1451 (2015).

27. R. Martin, "Noise power spectral density estimation based on optimal smoothing and minimum statistics," IEEE Trans. Speech Audio Process. **9**(5), 504-512 (2001).

28. Y. Ephraim and D. Malah, "Speech enhancement using a minimum mean-square error short-time spectral amplitude estimator," IEEE Trans. Acoust. Speech Signal Process. ASSP, **32**(6), 1109-1121 (1984).

29. A. D. Ball, G. D. Buckwell, "Chi squared distribution," (Macmillan Education UK, London, 2005).

30. M. T. Akhtar and W. Mitsuhashi, "Variable step-size based method for acoustic feedback modeling and neutralization in active noise control systems," Applied Acoustics, **72**(5), 297-304 (2011).